Iranian Journal of Medical Physics
Vol. 13, No. 2, June 2016, 125-136
Received: October 25, 2015; Accepted: May 02, 2016

Original Article

The Experimental Study of Increased ICP on Cerebral Hemorrhage Rabbits with Magnetic Induction Phase Shift Method

Jian Sun[1], Gui Jin[2], Gen Li[3], Yujie Chen[1], Mingxin Qin[2*], Hua Feng[1]*

Abstract

Introduction
Measuring magnetic induction phase shift (MIPS) changes as a function of cerebral hemorrhage volume has the potential for being a simple method for primary and non-contact detection of the occurrence and progress of cerebral hemorrhage. Our previous MIPS study showed that the intracranial pressure (ICP) was used as a contrast index and found the primary correlation between MIPS and ICP.
Materials and Methods
In this study, we theoretically deduced the approximate relationship between MIPS and ICP and carried out a comparison study between MIPS and ICP on cerebral hemorrhage in rabbits in this study. Acute cerebral hemorrhage was induced by injecting autologous blood (3 to 6mL) into the brain of rabbits in the experimental group (n=7).
Results
The animal experiment results showed that the MIPS decreased significantly as a function of injection volume in the experimental group and the changes of ICP and MIPS of rabbits from experimental group presented a negative correlation. We also found that the MIPS slopes of all experimental samples had a change trend from fastness to slowness with a reverse of the change of ICP.
Conclusion
These observations suggested that the non-contact MIPS method might be valuable and potential for monitoring acute cerebral hemorrhage and obtaining the ICP information.

Keywords: Intracranial Pressure, Cerebral Hemorrhage, Magnetics, Electromagnetic Fields

1. *Department of Neurosurgery, Southwest Hospital, Third Military Medical University, No.29 Gaotanyanzheng Street, Shapingba District, Chongqing 400038, China*
*Corresponding author: Tel: +86-17092320898; Fax: +86-23-68771267; E-mail: 30067982@qq.com

2. *College of Biomedical Engineering, Third Military Medical University, No. 30 Gaotanyanzheng Street, Shapingba District, Chongqing 400038, China*
*Corresponding author: Tel: +86-13256895471; E-mail: 1306542011@qq.com

3. *College of Bioengineering, Chongqing University, No. 174 Shazheng Street, Shapingba District, Chongqing40044, China*

1. Introduction

Magnetic induction phase shift (MIPS) has been used to study the water content of the brain, dielectric constant, brain hematoma, and cardiopulmonary activities [1-4]. As shown by Tarjan and McFee [5], electrodeless measurement of changing impedance in the human body may be facilitated by analyzing the effect of induced eddy currents.

According to the literature, different biological tissues have diverse electromagnetic properties, which allow them to be distinguished from each other [6]. A method for measuring changes in electromagnetic properties is to employ two non-contact induction coils placed around the tissue; this technique could be an alternative approach for the detection of clinical changes [7, 8].

In particular, MIPS changes across time after the occurrence of a suspected clinical episode could serve as a first-order clinical warning sign for detecting the presence and progression of such changes [9]. In the literature, volumetric inductive phase shift method has been used for breast cancer detection. The results suggest that this technique has the potential to detect pathological conditions associated with cancer in breast tissues through non-invasive monitoring [10].

In the present research, the purpose of MIPS study was to assess the electromagnetic properties of biological tissues. In previous research, we conducted a systematic study of brain monitoring through MIPS method, which comprised of theoretical calculations, use of an excitation source, detection sensor, and phase detector, a cerebral edema nerve cell model, a physical model of cerebral edema, and utilization of an experimental system. By using the detection system and the physical model of cerebral edema, an experimental simulation was performed to detect cerebral edema [11, 12].

According to the findings of the above-mentioned studies, MIPS was directly proportional to the volume, conductivity, and frequency in the physical model of cerebral edema. The MIPS method was suggested to have the potential for cerebral edema detection. Furthermore, in 2014, a special phase detector was designed for MIPS measurement of cerebral hemorrhage, which could distinguish minimal cerebral hemorrhage with a volume of approximately 0.5 ml [13].

In addition, in a previous study, considering the symmetry between the two brain hemispheres, a symmetric cancellation-type sensor detection system was designed to improve the detection sensitivity of MIPS [14]. In this study, the average phase drift induced by a 3-ml injection of autologous blood was 1.885° [14].

In order to study a wider band of MIPS detection and to provide more useful information for the measurement of cerebral hemorrhage, we established an MIPS spectroscopy (MIPSS) detection system for cerebral hemorrhage. The average phase shift induced by the 3-ml injection of autologous blood under the feature band was -7.7503±1.4204°, which was considerably higher than the value reported in our previous study [15].

In 2014, based on the abovementioned study, we carried out an experiment for the detection of acute cerebral hemorrhage (ACH) [16]. In this experiment, ACH was induced in six rabbits by injecting autologous blood at a speed of 0.33 ml/min. The intracranial pressure (ICP) and heart rate (HR) of subjects were monitored for about 1 h. Our results showed a significant increase in MIPS as a function of injection volume, which was consistent with the simulation test results.

In our previous study [16], ICP measurement was used as an important criterion in animal experiments. Based on the findings, MIPS was significantly related to ICP. For further clarification, we attempted to provide a theoretical explanation by utilizing non-contact measurement of the electromagnetic properties of the brain. A relationship was identified between MIPS and ICP by performing experiments on induced ACH in the rabbit brain. In addition, we discussed the possibility that MIPS could reflect ICP-related information.

While ICP monitoring has been used for decades as the most important index of patient condition in fields of neurosurgery and neurology, this type of bedside monitoring is invasive and expensive for patients. Therefore, a new cost-effective and non-contact method could be used for determining patient condition in neurosurgery and neurology if a relationship between MIPS and ICP could be established. In this study, we aimed to describe the theoretical calculations, experimental devices, and results obtained by evaluating ACH in the brain of rabbits.

2. Materials and Methods

2.1. Relationship between MIPS and ICP

A head model was built upon an anatomic base (Figure 1). The volume and total average conductivity of the model are denoted by V and $\bar{\sigma}$, respectively. The head model was divided into three parts: skull, cerebrospinal fluid (CSF), and combination of cerebral blood and brain (BB).

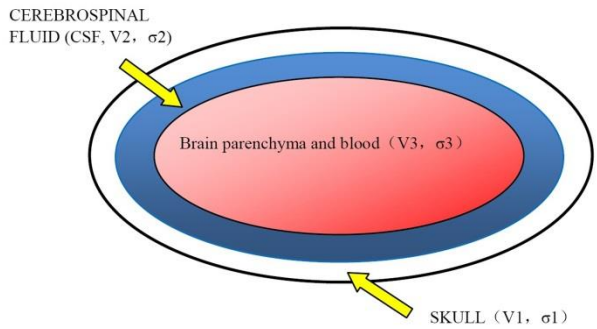

Figure 1. The electrical conductivity distribution in the rabbit head model; we developed the head conductivity model (V denotes the volume). The head is divided into three parts: skull (V1, σ1), cerebrospinal fluid (V2, σ2), and the combination of cerebral blood, brain white matter, and gray matter (V3, σ3). Under normal conditions of the brain, the total volume of the head model and its average conductivity remain unchanged.

Under normal conditions of the brain, the total volume of the head model and its total average conductivity remained unchanged. In this model, it was assumed that the average conductivity in each part is uniformly distributed. The total average conductivity $\bar{\sigma}$ of the model was calculated as follows:

$$\bar{\sigma} = \frac{V_1}{V}\sigma_1 + \frac{V_2}{V}\sigma_2 + \frac{V_3}{V}\sigma_3 \quad (1)$$

where V_1, V_2, and V_3 denote the volume of the skull, CSF, and BB, respectively, and conductivity in the skull, CSF, and BB is denoted by σ_1, σ_2, and σ_3, respectively.

According to Harvey Cushing' doctrine of an intact skull [17], increased ΔV in the bleeding volume of ACH causes a decline in ΔV of CSF. Therefore, the total average conductivity of the ACH model was calculated as follows:

$$\bar{\sigma}' = \frac{V_1}{V}\sigma_1 + \frac{V_2 - \Delta V}{V}\sigma_2 + \frac{V_3 + \Delta V}{V}\sigma_3 \quad (2)$$

Also, the total average conductivity change $\Delta\bar{\sigma}$ of the model was calculated as follows:

$$\Delta\bar{\sigma} = \bar{\sigma}' - \bar{\sigma} = \frac{\Delta V}{V}\sigma_3 - \frac{\Delta V}{V}\sigma_2 \quad (3)$$

The constant C was defined as:

$$C = \frac{V}{\sigma_3 - \sigma_2} \quad (4)$$

By integrating Equation (4) into Equation (3), the bleeding volume was expressed as:

$$\Delta V = C\Delta\bar{\sigma} \quad (5)$$

According to Cushing's doctrine, the volume-pressure curve could be approximately expressed as:

$$P = P_0 e^{K\Delta V} \quad (6)$$

When the content volume of the cavity showed an increment in ΔV, ICP and volume showed the above relations which was shown in Equation (6). In Equation (6), P_0 is the normal ICP and K is a constant value.

By integrating Equation (5) into Equation (6), the relationship between ICP and the change in total average conductivity was described as follows:

$$P = P_0 e^{KC\Delta\bar{\sigma}} \quad (7)$$

The volume-pressure and volume-conductivity curves are presented in Figure 2 after incorporating the electrical properties of brain tissues into Cushing's doctrine [17]. According to Griffiths [18], MIPS (Δθ) is proportional to $\Delta\bar{\sigma}$ and is calculated as follows:

$$\Delta\theta \approx \left|\frac{\Delta B}{B}\right| \propto \omega \Delta\bar{\sigma} \quad (8)$$

where B and ΔB are the primary and secondary magnetic fields, respectively, and ω is the angular frequency of a sinusoidal excitation.

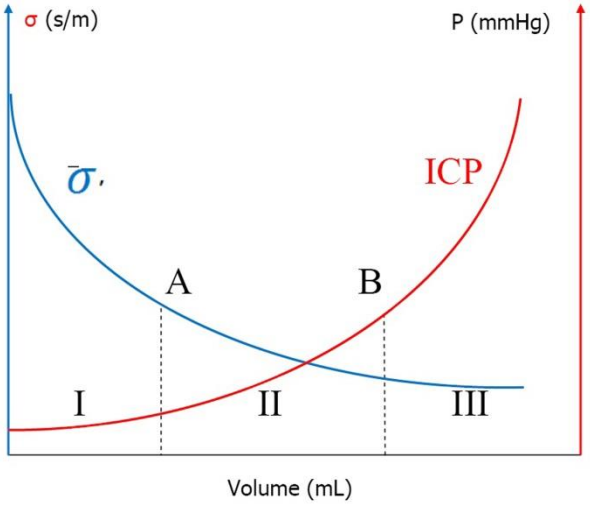

Figure 2. The relationship between volume, ICP, and brain conductivity. The ICP curve is characterized by an increase due to elevated blood volume; however, the change in the average conductivity of the brain is the opposite. When the content volume of cranial cavity showed a small increment in ΔV, the average conductivity $\bar{\sigma}'$ would fall $\Delta\bar{\sigma}$ according to Equation (3).

Equation (8) was integrated into Equation (7):

$$P = P_0 e^{KA\Delta\theta} \quad (9)$$

where P_0 is the normal ICP and K and A are constant values.

As MIPS (Δθ) was measured experimentally with our detection system, MIPS corresponded to ICP in Formula (9). The difference between the two measured MIPS values was used if a dynamic change was observed in MIPS.

According to Formula (3) and the lower conductivity of BB (σ_3), compared to CSF (σ_2), $\Delta\bar{\sigma}$ was determined to be below zero. Therefore, when the content volume of cranial cavity showed a small increment in ΔV, the average conductivity $\bar{\sigma}'$ would fall $\Delta\bar{\sigma}$ according to Equation (3).

As presented in Figure 2, the increase in ICP was categorized as follows: Phase I, Phase II, and Phase III.

In classes I and II, the change in brain conductivity was significant, while the shift in ICP was trivial. However, in class III, the change in brain conductivity was slow, while the change in ICP was major. As stated in Harvey Cushing's doctrine, such observation is attributed to the compensatory effect of the intracranial material balancing the ICP increase in areas I and II, while the compensatory effect was not reported in area III.

2.2. MIPS experimental setup

The MIPS experimental setup was designed and constructed, consisting of seven modules: signal generator, excitation coil, detection coil, phase detector, personal computer (PC), and parts responsible for biological signal collecting and processing. The system block diagram is presented in Figure 3.

The signal generator (self-made) supplied a sinusoid signal V_e of 5 V at 10.7 MHz. The magnetic strength was weak for our coils. In the present study, rabbit brains were assessed, and consequently, the coils fitted the corresponding size of the brain. The excitation and detection coils were coaxially placed. The two coils comprised of ten turns of magnetic wire with a radius of 5 cm, and the distance between the coils was 11 cm.

The excitation coil induced a current in the detection coil through magnetic induction. The phase shift between the excitation and detection signals was measured by our phase detector, which integrated a pre-amplifier (range: 0-33 dB) and a filter. The signal-to-noise ratio was improved and we were able to detect very weak signals.

Performance measurements confirmed that the phase noise and drift were very low, thus satisfying the requirements of this study. The electrocardiograph (ECG) and ICP data collection device (Model 6280C, Chengdu Instrument Factory, CHINA) were controlled by the PC (Dimension 8300, Dell Inc., USA).

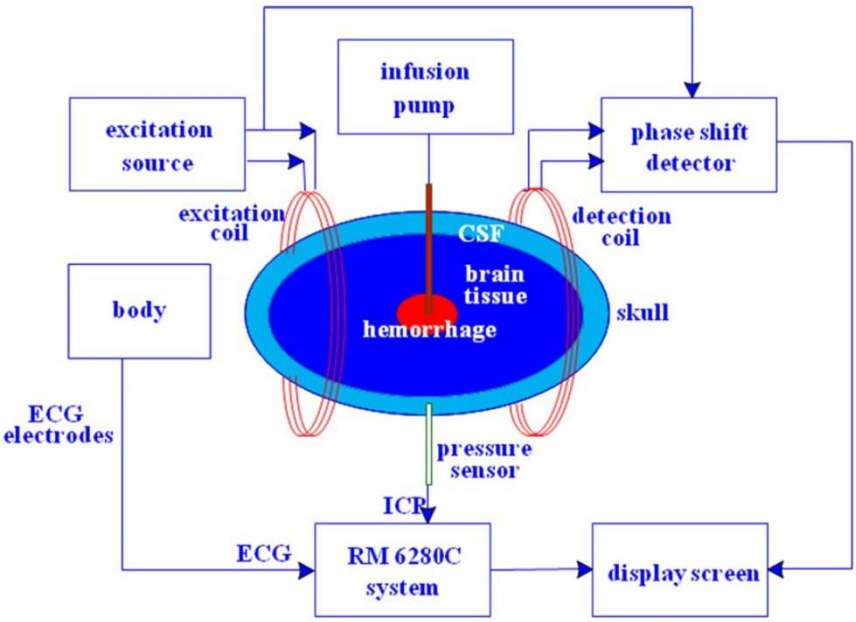

Figure 3. The system block diagram of the MIPS detection method. The data obtained from the rabbits included MIPS, HR, and ICP. These data were synchronously collected for comparing MIPS with ICP.

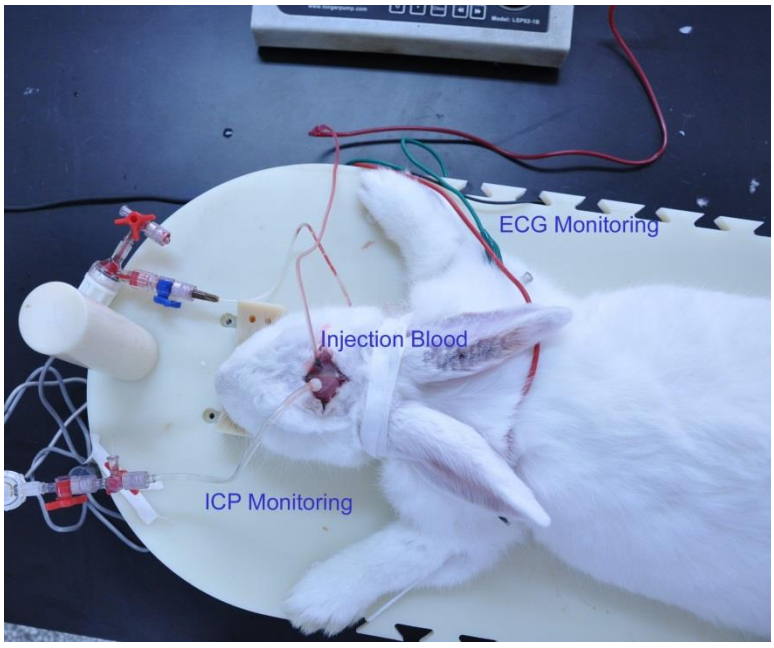

Figure 4. The rabbit model of acute cerebral hemorrhage (ACH). The model was established by means of stereotactic methods [16].

2.3. Surgical Procedure and Data Processing

Seven rabbits from the experimental group (weight range: 2.2-3.5 kg, mean weight: 2.5±0.2 kg) and four rabbits from the control group (weight range: 2.3-2.7 kg, average weight: 2.4±0.2 kg) were anaesthetized with urethane (25%, 5 ml/kg) through the ear vein. We established the ACH model, using stereotactic methods [16]. Autologous blood (3-6 mL) was injected in the rabbits of the experimental group at a speed of 0.33 ml/min. The physiological signal collection device (RM6280C, Chengdu Instrument Factory) was used to measure the changes in ICP and HR, as shown in Figure 4 [16]. The Animal Ethics

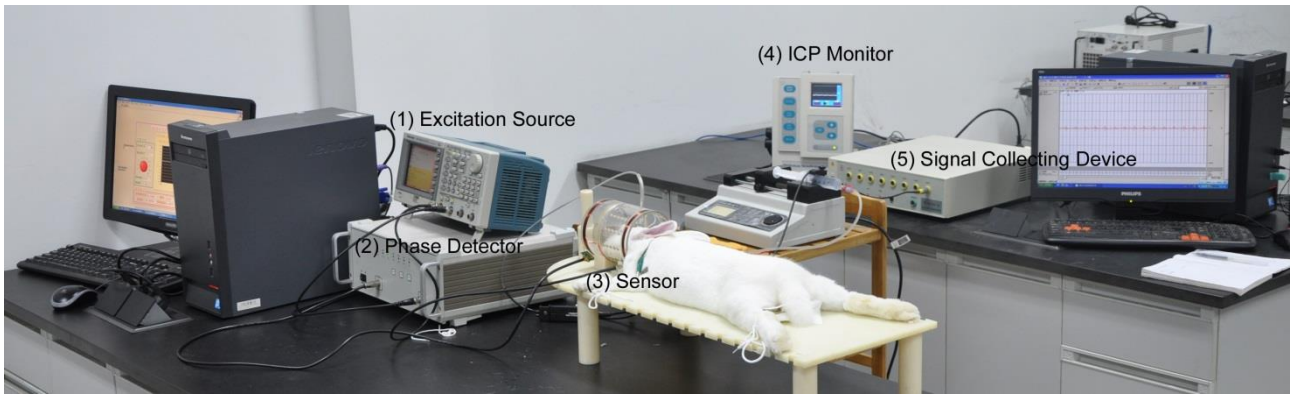

Figure 5. The experimental setup for the detection of ACH in rabbits through the MIPS method. The excitation and detection coils were coaxially placed. (1) Excitation source, (2) phase detector, (3) sensor, (4) ICP monitor, (5) signal collecting device.

Committee of the university approved all experimental protocols, and the procedures were carried out in accordance with the Declaration of Helsinki and the International Association for the Study of Pain (IASP) guidelines [19, 20].

Figure 5 shows the experimental setup for the detection of ACH in rabbits. ICP, HR, and MIPS were synchronously collected for the comparison of the results. Changes in MIPS were recorded with respect to the baseline obtained under normal conditions for rabbits after the surgical procedure. Experimental excitation and detection coils were coaxially placed around their heads. In all experiments, the head was centered between the excitation and detection coils.

Figure 6 shows the obtained data related to ACH in a rabbit (S20121213) in a typical experimental process. These signals were continuously monitored for 866 s. Injection of autologous blood into the brain started at 120 s until the end of the experiment; the injection speed was 0.33 ml/min. The ICP and ECG sampling rate was 1000 Hz, whereas that of MIPS was approximately 0.2 Hz.

The phase detector measured MIPS for 3 min and collected about 36 data points as each 1 mL blood injection was completed. To facilitate data analysis, the HR and ICP signals were down-sampled at 1 Hz, and the MIPS signal was re-sampled with a cubic spline interpolation.

3. Results

As presented in Figures 6 and 7, the signals were divided into four phases: I, II, III, and IV. HR was stable from 0 to 500 s. In phase I (from 0 to 120 s), ICP and MIPS in the experimental and control groups showed similar changes (±1 mmHg and ±0.005 degrees, respectively). In stage II (from 120 to 250 s), ICP changed from 9 to 20 mmHg, corresponding to the change in MIPS from 0.4 to 0.2 degrees.

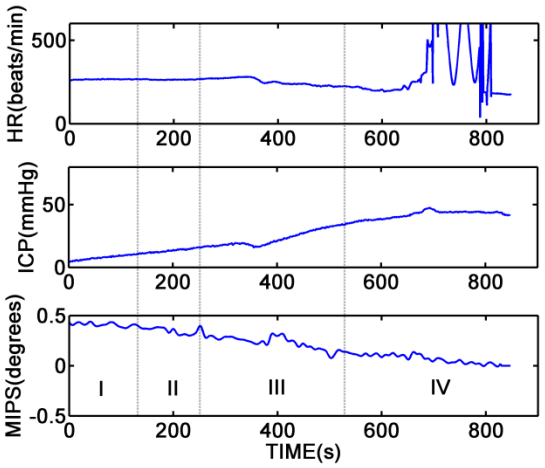

Figure 6. Data on the experimental setup for the detection of MIPS and the physiological signal collecting device (ACH rabbit S20121213 of the experimental group). The data obtained from the rabbits included MIPS, HR, and ICP. These data were synchronously collected for comparing MIPS with ICP.

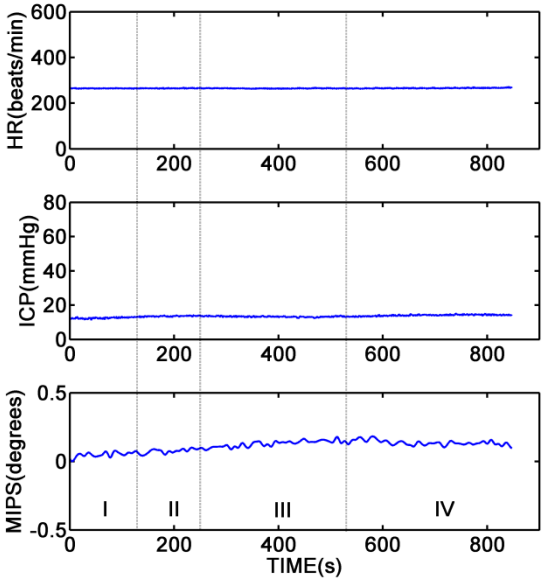

Figure 7. Data on the experimental setup and the physiological signal acquisition device (HR, MIPS, and ICP; normal rabbit S20130114 of the sham-operated control group)

For the experimental group (e.g., subject S20121213), the injection volume was nearly 0.7 mL (from 120 to 250 s). Due to CSF regulation by the intracranial material compensatory effect, ICP increased, while MIPS declined. With the increase in the injection volume, ICP began to rise and CSF started to exit the brain. Considering the compensatory effect of CSF, ICP only showed a small rise. However, MIPS was highly sensitive in this range and the slope greatly changed.

As presented in Figures 6 and 7, the signals were divided into four phases: I, II, III, and IV. HR was stable from 0 to 500 s. In phase I (from 0 to 120 s), ICP and MIPS in the experimental and control groups showed similar changes (±1 mmHg and ±0.005 degrees, respectively). In stage II (from 120 to 250 s), ICP changed from 9 to 20 mmHg, corresponding to the change in MIPS from 0.4 to 0.2 degrees.

For the experimental group (e.g., subject S20121213), the injection volume was nearly 0.7 mL (from 120 to 250 s). Due to CSF regulation by the intracranial material compensatory effect, ICP increased, while MIPS declined. With the increase in the injection volume, ICP began to rise and CSF started to exit the brain. Considering the compensatory effect of CSF, ICP only showed a small rise. However, MIPS was highly sensitive in this range and the slope greatly changed.

Since CSF showed the highest conductivity in the brain, CSF compensation regulation had a significant effect on the overall average conductivity. With the decline in CSF volume, the overall average conductivity of the brain began to reduce and MIPS showed a major decline. Phase III was the range of cerebral blood volume compensation regulation (from 250 to 520 s).The ICP began to rise rapidly to 60 mmHg and MIPS changed from 0.2 to 0.1 degrees.

In the experimental group (e.g., subject S20121213), the injection volume was nearly 1.4 mL (from 250 to 520 s). Cerebral blood volume regulation dominated this compensatory range and its regulatory ability was obviously less significant than CSF. Since compensatory regulation was eventually exceeded, ICP showed a major rise with the increase in injection volume.

Given the less significant change in the cranial content and the smaller conductivity of cerebral blood than CSF, the sensitivity of MIPS subsequently decreased and its slope began to slowly change. As the findings revealed, phase IV was more complicated (from 500 s to the end). As shown in Figure 6, HR abruptly increased and fell, and the vital signs became unstable. Therefore, ICP showed a dramatic fluctuation, whereas the MIPS slope changed steadily.

We performed paired t-test for the evaluation of ICP and MIPS of seven rabbits from the experimental group. The corresponding t-values of MIPS and ICP were 4.923 and 7.405 with probabilities of P_{ICP} = 0.008 and P_{MIPS} = 0.002, respectively (P=0.01). Both MIPS and ICP of the experimental group were significantly different from the control group. Figure 8 shows the MRI results in the experimental and control groups. The ACH regions are circled in red at the brain parenchyma in Figure 8B.

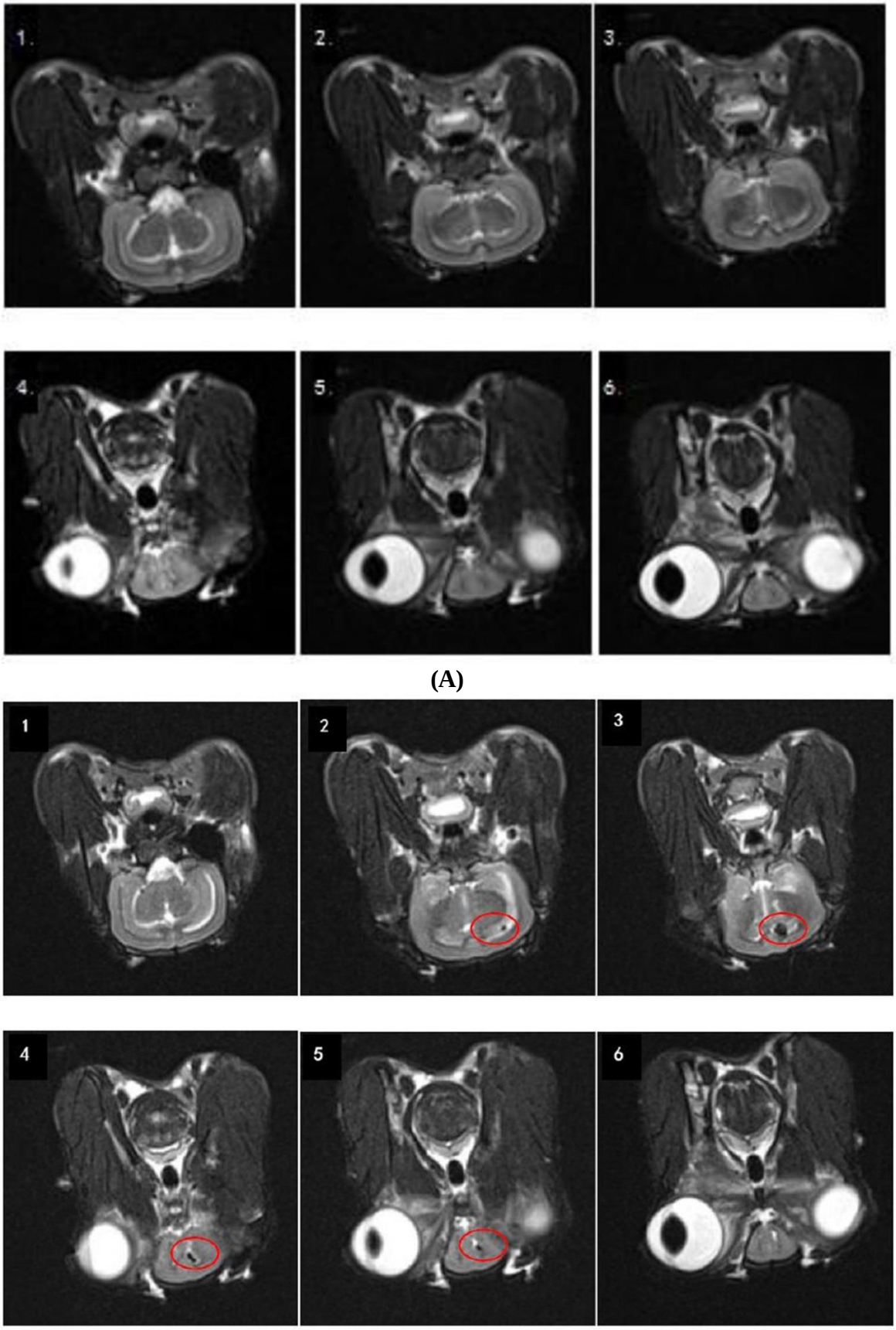

Figure 8. A) Brain MRI of one rabbit from the control group. B) Brain MRI of a rabbit with ACH. ACH regions are circled in red at the brain parenchyma.

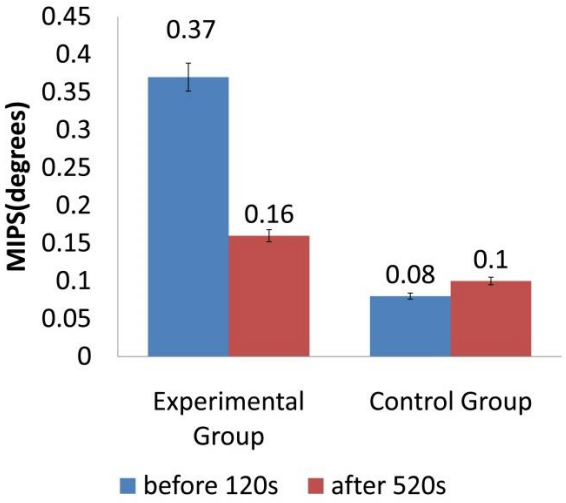

Figure 9. The change of MIPS in the experimental and control groups. The average value of MIPS in seven rabbits from the experimental group fell from 0.37 to 0.16 degrees, with the injection volume increasing from zero to about 2.22 ml. For the control group, MIPS changed from 0.08 to 0.1 degrees.

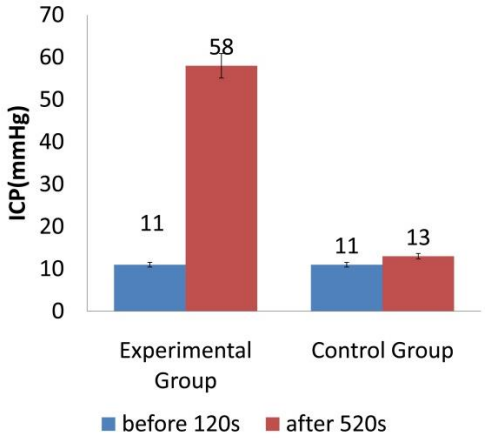

Figure 10. The change of ICP in the experimental and control groups. The average ICP in seven rabbits from the experimental group rose from 11 to 58 mmHg with the injection volume rising from zero to about 2.22 ml. In the control group, ICP changed from 11 to 13 mmHg.

The MIPS and ICP data were analyzed when HR was stable in rabbits. Changes in MIPS and ICP in the experimental and control groups are shown in Figures 9 and 10. The average MIPS of seven rabbits from the experimental group fell from 0.37 to nearly 0.16 degrees, while the injection volume rose from 0 to about 2.22 ml, as demonstrated in Figure 9. Therefore, MIPS dropped by 0.095 degrees, while ICP increased by 21.17 mmHg (1 ml bleeding).

Figures 9 and 10 also show that MIPS changed from 0.08 to 0.1 degrees in four rabbits from the control group due to a temperature drift. The slow increase in the ICP of the control group could have been caused by a spontaneous intracerebral hemorrhage or cerebral edema in the craniotomy; accordingly, MIPS might have dropped by 0.095±0.0035 degrees (1 ml bleeding). By excluding the influence of temperature drift from the MIPS detection system, the MIPS value would be larger.

4. Discussion

Figure 11 shows the MIPS slope in the experimental group. It is clear that the MIPS slope in all the samples ran from high to low. This tendency supports our assumption that MIPS is more sensitive in the early stage of ACH. The slope of ICP changed from moderate to steep and was contrary to the change in MIPS. We can draw the conclusion that our method may be used to monitor ACH. Changes in ICP and MIPS in seven rabbits of the experimental group had a negative correlation, and the corresponding values ranged from 0.50804 to 0.90914.

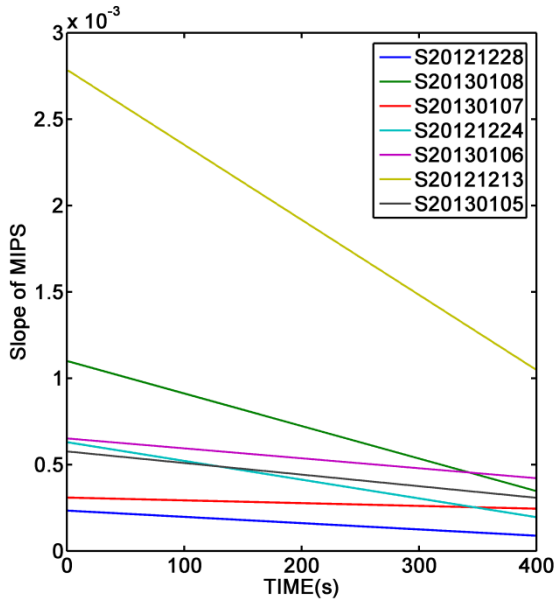

Figure 11. The slope of MIPS in the experimental group. The average slope for seven rabbits ranges from $1.6079 *10^{-4}$ to $1.9076*10^{-4}$.

The shift in MIPS might reflect a change in CSF and cerebral blood volume, as previously reported in the literature [9-16]. Our MIPS system was able to detect the volume of ACH with a non-invasive and non-contact method. The comparison of analytical and experimental results with previous studies [7-9] suggests that various physiological conditions in the brain, such as edema and ischemia, can be distinguished through the analysis of MIPS change at specific frequencies.

Edema development after ACH can elevate ICP and cause herniation, brain stem compression, and death [17]. Clinical studies have demonstrated that the maximum rate of ACH-induced death occurs within the first few days following ictus and is likely to be associated with progressive edema development [21-24]. Since edema is nearly maximal at 24 h after ACH, therapy directed at reducing edema formation must be initiated on the first day [25].

In our experiments, the volume of edema changed insignificantly within a short time span (about 900 s) and there were no noticeable changes in MIPS in the control group; therefore, the change in MIPS was mainly a consequence of ACH. Considering the brain damage, spontaneous cerebral hemorrhage, and cerebral edema, the blood volume flow rate was approximately 100-300 µl (individual differences) in less than 1 h after craniotomy [26]. Overall, an animal hemorrhage model should consider spontaneous intracerebral hemorrhage; it should be noted that the cerebral perfusion pressure remained mainly unchanged.

We also performed simulation studies, using the finite element method (FEM). MIPS dropped by 0.026 degrees with 2.22 mL bleeding. The results showed that MIPS changes were a function of volume for the simulated hemorrhage conditions. The experimental results were not on the same order of magnitude as the simulation results.

While the observed difference could be attributed to various factors, the main reason is the use of a simplified brain model. The comparison with FEM simulation and our previous salt simulation studies [15, 16] suggests that a simple brain model could show similar MIPS changes and the results would be still different from the actual findings. Accordingly, in future studies, we aim to develop a more comprehensive brain model.

5. Conclusion

Measurement of MIPS changes is potentially a simple method for primary and non-contact detection of the occurrence and progression of cerebral hemorrhage. This method is useful in emergency medicine, critical care, and other clinical fields; additionally, the applied device is small and portable.

This study sought to reveal the relationship between MIPS and ICP changes, using an animal model. We deduced the theoretical relationship between conductivity and ICP ($P = P_0 e^{K A \Delta\theta}$), based on the brain model. We verified our observations according to the experimental results. In this study, we proposed a novel hypothesis, which still has some deficiencies. Biological tissues lack uniform conductivity distribution, and the geometric size determining the surrounding electromagnetic field is not static. Therefore, the next step is to improve the theoretical model and attempt to solve this shortcoming.

In this study, the curve of changes in MIPS was significantly related to the changes in ICP. This observation suggests that the applied method could be valuable in emergency medicine as an early indicator. Moreover, this method could be applied in geriatric medicine for homebound debilitated individuals, diagnostic ultrasound imaging of the fetus, ICP measurements and continuous monitoring in critical care units, and assessment of unconscious patients in ICUs. This study also suggests that MIPS could be used in studies on monkeys and dogs.

Numerous factors are involved in the increase in ICP. The MIPS method could not identify all intracranial pressure factors, which need to

be assessed. Therefore, we need to perform a comparative study of cerebral hemorrhage and cerebral edema. We hope to improve the operating speed of the phase detector in order to achieve real-time monitoring of MIPS (<5 ms), based on the National Instruments-PCI Extensions for Instrumentation (NI-PXI).

To improve the rabbit experiments, we need to examine different bleeding positions, induce cerebral edema, and use large samples. We plan to use imaging methods to demonstrate the regulating effects of CSF and cerebral blood. This experiment was only a theoretical research into conductivity and ICP change. In future studies, we aim to identify feature points of slow to rapid changes in ICP and calculate the threshold in order to facilitate the use of these findings in clinical applications. This study was a preliminary research, and further analysis is required to confirm our observations.

Acknowledgments

There was no conflict of interest to be declared. This study was supported by the National Natural Science Foundation of China (61072254) and the Science & Technology Research Project Foundation of CHONGQING (CSTC2012GG-YJS10013).

References

1. Scharfetter H, Cabanas R, Rosell J. Biological Tissue Characterization by Magnetic Induction Spectroscopy (MIS) Requirements and Limitations. IEEE T Bio-Med Eng. 2003 Jul; 50(7): 870-80.
2. Ragauskas A, Daubaris G, Ragaisis V, Petkus V. Implementation of Non-invasive Brain Physiological Monitoring Concepts. Med Eng Phys. 2003 Oct; 25(8): 667-8.
3. Steffen M, Heimann K, Bernstein N, Leonhardt S. Multichannel simultaneous magnetic induction measurement system (MUSIMITOS). PHYSIOL MEAS. 2008 Jun; 29(6): 291-306.
4. Rojas R, Rubinsky B, Gonzalez CA. The effect of brain hematoma location on volumetric inductive phase shift spectroscopy of the brain with circular and magnetron sensor coils: a numerical simulation study. PHYSIOL MEAS. 2008 Jun; 29(6): 255-66.
5. Tarjan PP, McFee R. Electrodeless measurements of the effective resistivity of the human torso and head by magnetic induction. IEEE T Bio-Med Eng. 1968 Oct; 15(4): 266-78.
6. Foster KR, Schwan HP. Dielectric properties of tissues and biological materials: a critical review.CRIT REV BIOMED ENG. 1989; 17(1): 25-104.
7. Gonzalez CA, Rubinsky B. A theoretical study on magnetic induction frequency dependence of phase shift in oedema and haematoma. PHYSIOL MEAS. 2006 Sep; 27(9): 829-38.
8. Gonzalez CA, Rubinsky B. Detection of brain oedema with frequency dependent phase shift electromagnetic induction. PHYSIOL MEAS. 2006 Jun; 27(6): 539-52.
9. Gonzalez CA, Villanueva C, Vera C, Flores O, Reyes RD, Rubinsky B. The detection of brain ischaemia in rats by inductive phase shift spectroscopy. PHYSIOL MEAS. 2009 Aug; 30(8): 809-19.
10. Gonzalez CA, Lozano LM, Uscanga MC, Silva JG, Polo SM. Theoretical and Experimental Estimations of Volumetric Inductive Phase Shift in Breast Cancer Tissue. J PHYS CONF SER.2013; 434: 012004.
11. Xu L, Qin MX, Jin GNing X, Xu J. Study of PSSMI for cerebral hemorrhage detection: an experimental simulation. 4thIntConf on Image and Signal Processing. 2011; 1: 266-8.
12. Jin G, Qin MX, Wang CGuo WY, Xu L, Ning X, et al. Experimental study on simulated cerebral edema detection with PSSMI.IntConf on Electric and Electronics. 2011; 100: 361-7.
13. Jin G, Sun J, Qin MX, Wang C, Guo WY, Yan QG, et al. A Special Phase Detector for Magnetic Inductive Measurement of Cerebral Hemorrhage.PLOS ONE, 2014; 9(5): e97179.
14. Jin G, Sun J, Qin MX, Tang QH, Xu L, Ning X, et al. A new method for detecting cerebral hemorrhage in rabbits by magnetic inductive phase shift. BIOSENSBIOELECTRON. 2014; 52: 374-8.
15. Pan WC, Yan QG, Qin MX, Jin G, Sun J, Ning X, et al. Detection of Cerebral Hemorrhage in Rabbits by Time-Difference MagneticInductive Phase Shift Spectroscopy. PLOS ONE, 2015; 10(5): 0128127.
16. Sun J, Jin G, Qin MX, Wan ZB, Wang JB, Wang C, et al. Detection of acute cerebral hemorrhage in rabbits by magnetic induction. Braz J Med Biol Res, 2014; 47(2): 144-50.

17. Avezaat CJ, Vaneijndhoven JH, Wyper DJ. Cerebrospinal fluid pulse pressure and intracranial volume-pressure relationships. J NeurolNeurosur PS. 1979; 42(8): 687-700.
18. Griffiths H, Steward WR, Gough W. Magnetic induction tomography—a measuring system for biological materials. Ann NY Acad Sci. 1999 Apr; 873(20): 335-45.
19. Zimmermann M. Ethical guidelines for investigations of experimental pain in conscious animals.PAIN.1983 Jun 1; 16(2): 109-10.
20. Helsinki. Declaration of Helsinki. Brit Med J (BMJ). 1999 May; 357(9266): 1448-9.
21. Diringer MN. Intracerebral hemorrhage: pathophysiology and management.Crit Care Med. 1993 Oct; 21(10): 1591-603.
22. Ropper AH, King RB. Intracranial pressure monitoring in comatose patients with cerebral hemorrhage.Arch Neurol -Chicago.1984 Jul; 41(7): 725-8.
23. Broderick JP, Brott TG, Duldner JE, Tomsick T, Huster G. Volume of intracerebral hemorrhage: a powerful and easy-to-use predictor of 30-day mortality. STROKE.1993 Jul; 24(7): 987-93.
24. Jan C, Ricardo C, Kurt TK, Evelyn YD, Sander C, Stephan AM. Global cerebral edema after subarachnoid hemorrhage.STROKE.2002 Sep; 33(9): 2153-4.
25. YangGY, Lorris B, Chenevert TL, Brunberg A, Hoff JT. Experimental intracerebral hemorrhage: relationship between brain edema, blood flow, and blood-brain barrier permeability in rats. J Neurosurg.1994 Jul; 81(1): 93-102.
26. Nath FP, Jenkins A, Mendelow AD, Graham DI, Teasdale GM. Early hemodynamic changes in experimental intracerebral hemorrhage intracerebral hemorrhage.J Neurosurg.1986 Nov; 65(5): 697-703.